CRACK CLOSURE EFFECTS IN FATIGUE PROPAGATION OF ELLIPTICAL CRACKS

A. Clerivet*, C. Bathias*

Evidence is presented in this paper that the crack closure concept is not limited to the case of propagation under plane stress conditions. To achieve this objective tests were performed on tension and bending specimens containing surface or corner flaws. An aluminium alloy type 2124-T351 has been used in this work. The influence of various parameters such as, applied stress, R ratio, stress state and load variation (overload) on crack closure has been studied. The main conclusion is that a crack closure mechanism acts under plane strain conditions, whatever the parameter studied, even if other mechanisms are also effective.

INTRODUCTION

Studies on crack closure under plane strain propagation conditions are often carried out using compact tension (C.T.) specimens. However, both experimental techniques and interpretations of results have given rise to considerable controversy. This observation has been developed in a previous publication (1). Hence, a study of closure mechanism has been conducted on fatigue propagation of semi- (or quarter) elliptical cracks where a plane strain state is predominant. However, before discribing the influence of various parameters on the closure mechanism of such a crack, a summary of previous work conducted on central crack tension (C.C.T.) specimens is presented. This showed that crack closure variation in the plane stress states takes into account the major effect of variable amplitude loading. Semi-empirical relations have been derived from these results which are extrapolated to the case of elliptical cracks.

* Université de Technologie de Compiegne, France

EXPERIMENTAL PROCEDURE

Two plates, referred to as (A) and (B), of 2124-T351 aluminium alloy have been used for fabrication of the specimens. The chemical compositions are:

	Cu	Mg	Mn	Cr	Si	Fe	Ti	Zn
(A)	4.35	1.45	0.6	0.01	0.11	0.23	0.02	0.04
(B)	4.37	1.46	0.63	0.01	0.11	0.21	0.03	0.04

The mechanical properties are given in the following table:

Plate	(A)	(B)		
Direction	L.T.	L.	L.T.	S.T.
Yield Stress (MPa)	274	374	336	309
U.T.S. (MPa)	440	492	473	423
Elongation (%)	18	18	15	7

L. : longitudinal (rolling direction)
L.T.: long transverse
S.T.: short transverse.

Specimens type C.C.T. (200 mm wide, 1.6 mm thick) and type C.T. (width 75 mm, thick 12 mm) were machined out of the plate (A). Special specimens for tension and bending were machined from the other plate (B). In these specimens one semi-circular surface flaw or two quarter-circular flaws were created by means of an electro-discharge machine (figure 1). The tensile stress direction was LT.

A servo hydraulic fatigue machine controlled by a mini-computer was used for the overload tests. The cracks were propagated at a frequency of 10 Hz, during constant amplitude (C.A.) loading. One millimeter before application of an overload the frequency was changed to 0.1 Hz. A clip gage (gage length: 2.5 mm) was located ahead of the crack tip in the affected zone. Tests were continued at this frequency as the crack propagation is affected by the overload. In the case of C.A. loading tests the frequency was reduced to 0.1 Hz only for recording the load displacement diagrams. For all tests the baseline load amplitude was kept constant.

Surface crack lengths were measured by means of a travelling microscope. In the case of semi-elliptical cracks the front were reconstituted after specimens were broken. Different positions of the crack front are marked with coloured inks introduced into the crack during the test.

PART I

Overload influence on crack closure under plane stress propagation conditions.

Before the publication of Elber's concept (2) of crack closure, it was generally admitted that residual stresses associated with plastic zone interactions were responsible for the overloading effect (3). It seems, now, that residual deformations just behind the crack tip control the major part of the mechanisms of crack propagation (in plane stress) under variable amplitude loading. Yet, it is still not generally accepted (4), (5), (6). Evidence of the validity of the concept has been given in previous publications (7), (8). Various parameters such as overload ratio (τ_p), R-ratio, and initial loading have been examined in these previous studies. Results reveal that when the crack growth rate is reported as a function of ΔK_{eff} instead of ΔK, experimental points show a linear relationship (in a log-log graph) which corresponds to the Paris' relation determined under C.A. loading. For the example given in figures 2 and 3 the parameters are: $\Delta K_o \approx 12$ Mpa $\sqrt{m}$, $R = 0.01$, $\tau_p = 2$. However, this experimental evidence does not permit a prediction of the retardation due to overloading because the ratio U is no longer constant. The function cannot be determined mathematically from two relations as:

$$da/dN = C\ \Delta K^m \quad \text{and} \quad da/dN = C_E\ (U\ \ \Delta K)^m$$

In fact it was necessary to evaluate a function U of the variable a (crack length) according to parameters such as, overload ratio, plastic zone size, etc.

In reference (7) we showed that the crack growth increment necessary for the ratio U to recover its baseline value (U_o) is very close to the affected zone size. The latter has been correlated to the overload plastic zone size determined from Irwin's equation. In reference (8) a relationship was established between the minimum values by the U ratio and threshold values relative to overloads. Results indicated on one hand, that the U variation follows a power function of the variable and on the other hand, that the zone of delayed retardation was independent of the overload ratio (4), (8). This latter fact has been experimentally verified for various parameters (8). This zone has been related to the cyclic plastic zone size due to the baseline stress (8). The minimum value of U for any overload ratio, during the retarded crack growth period, is given by the relation:

$$U_m = U_o \left(\frac{1}{4\tau_p^2}\right)^{(\tau_p - 1)^\alpha}$$

where the coefficient α has been found to be dependent on the material properties (8).

The U variation, when the crack propagates outside the zone of delay retardation, is given by the following relationship:

$$U = U_o \left(\frac{a - a_o}{2r_{ymp}}\right)^{(\tau_p - 1)^\alpha} \quad \text{for} \quad 2r_{yco} \leq a - a_o \leq 2r_{ymp}$$

Results obtained by crack closure of threshold measurements for various parameters are reported in figure 4. We can see that experimental results verify such a parametric relationship.

Consideration of macroscopic and microscopic aspects of the mechanism of crack propagation in the affected zone has led us to take the initial value U_o as the value of U after overload. A relation is given as:

$$U = U_m \left(\frac{a - a_o}{2r_{yco}}\right)^k$$

where k is given by limits $U = U_o$ when $a - a_o = \Delta a_{p_1}$ and $U = U_m$ when $a - a_o = 2r_{yco}$. The crack growth Δa_{p_1}, due to the overload is determined from the crack closure level during the preceding cycles.

An example of the application of these relationships is given in figure 5. We can see that a prediction model based on crack closure is more realistic than a prediction model based on residual stress, for example Wheeler's model (3).

PART II

Closure effects in semi- (or quarter) elliptical cracks.

As reported previously results on crack closure obtained with C.T. specimens are often contradictory (1), (4). This is the reason that a study of crack closure under plane strain condition has been conducted on fatigue propagation of semi-elliptical cracks. It may be recalled that Elber (9) observed that crack closure does not differ for the two states of stress. Thus one or two micro-clip gages have been located just at the (surface) crack tip on tension specimens (surface or corner cracks). R-ratio values were 0.01 and 0.5. Results show (cf. figure 6) that, in the case, i.e. the clip gage just behind the crack tip, the crack closure level is found to be identical to that observed on C.C.T. specimens, for two R-ratios. An Elber's type relation has been established as $U = 0.45 + 0.4\ R$. It is clear that, in this case, information corresponds essentially to the response of a region of the specimen limited to the free surface, proof, a priori, of the validity of Elber's work. However, differences in load-displacement records are observed (cf. figure 7) as the crack propagates. A decrease of the crack closure stress to another value is noted, for two R-ratios. A new relationship has been established as $U_a = 0.7 + 0.4\ R$ which is in good agreement with relationships given by (10), (11) for aluminium alloys. These results confirm the mechanisms of closure defined from results on C.T. specimens: the crack closes gradually from the free surface to the center of the specimen. Thus it seems from these results that the crack closure level under plane strain conditions is no longer ambiguous. Two questions can now be formulated: does the ΔK_{eff} variation take into account the R-ratio effect under plane strain conditions and does it explain the influence of the stress state on the crack propagation, since two different closure levels have been found according to the two states of stress?

Difficulties have been encountered in the study of the influence of these parameters on crack growth rate as there is no general solution to determine the K variation all along the front of a semi- (or quarter) elliptical crack in cases of loading in tension or bending. The most completed formulations, at present, are given by Newman and Raju (12), (13). However, these formulations are based on the fact that the evolution of the crack fronts is given by a simple relation with respect to the loading mode. Our results (4) show that all parameters such as the applied stress and the R-ratio influence the evolution of the crack front. Thus as many relations between crack growth rate and ΔK can be found as there are loading parameters, at least for the crack growth determined at the surface (cf. figure 8). It seems, on the contrary, that these formulations can be used to determine the factor K at the furthest point of the crack front. Figure 9 shows that all the experimental points fall in a scatter band determined by using C.T. specimens. Similar results have been obtained from Kobayashi's relation, for two R-ratios (4). Thus, since a simple relation can be established (in plane strain condition) for a given R-ratio, the influence of this ratio can be studied in terms of ΔK_{eff}. Results are given in figures 10 and 11. They show that, when crack growth rate is reported as a function of ΔK_{eff}, using the above mentioned relation, $U_a = f(R)$, instead of ΔK a unique relationship is established whatever the R-ratio. Hence, evidence is presented that R-ratio influence is taken into account by a crack closure concept, not only under plane stress conditions, as usually reported, but also under plane strain conditions of propagation, at least in a region limited to the Paris' relation. However, a difference from Elber's work exists in the fact that the crack closure ratio is found to differ for the two states of stress at a given R-ratio. Thus, as this stress state plays a major role in crack growth rate can it be taken into account by a difference on crack closure level?

To answer this question and, as mentioned above, it was necessary to ensure that differences in crack growth were due to Newman's formulation. Calculations of K factors for eight fronts (three applied bending stresses) have been performed by (14). Results are given in figure 8 in comparison with those obtained from Newman's formulations. They show on one hand that an unique relation results and on the other hand that experimental results fall in a scatter band determined from C.C.T. specimens. Thus we may compare in ΔK_{eff} results obtained from C.T. and C.C.T. specimens. Results are given in figure 12. We can see that the major effect of stress state on crack growth rate can be explained by K_{eff} variation; a result which cannot be obtained from C.T. specimens alone.

Overload effect

Overload tests have been carried out on tension and bending specimens. Crack closure variation (at the surface) have been shown (4). Two examples of overloading tests are given in figures 13 and 14. The first example (tension) shows that there are variations of the crack growth rate before the crack propagates outside the affected zone. This phenomenon can be explained by the action of two principal mechanisms. The first mechanism is due to a crack closure effect which is predominant at the free surface. The second mechanism is due to a modification of the crack front which plays a prominent role in determining the intensity of the local stress. Retardation is less important for the major part of the crack front (interior of the specimen) than for a part of the crack front near to the free surface. When the part of the front in a plane strain state is no longer affected there is still an effect on the other part. Hence the crack front is modified such that the ellipse ratio (c/a) decreases. As a consequence the ratio K_c/K_a increases and therefore crack growth at the surface increases. Thus the ratio c/a increases, consequently the ratio K_c/K_a decreases and crack growth at the surface is decreased to a value inferior to that shown in uniform loading because the crack is still affected in this region. The phenomenon is observed until the part of the crack front in plane stress is no longer affected by the overload. After that we suppose that the evolution of the crack front is identical to that observed under C.A. loading.

Unfortunately the width of the specimens does not permit such an observation. From these facts we think that relations defined previously are applicable at least at the surface. Results are given in figures 13 and 14. Prediction is based on a Paris relation determined from C.A. loading (tension or bending). Hence a change of the crack front geometry due to overloading, as experimentally observed, is not taken into account. In spite of this fact we think that a closure model can explain the major effect of overloading. Other effects are due to crack front changes which affect the ratio K_c/K_a. However, it is not possible to take into account this phenomenon without a long numerical calculation as these is no valid formulation to determine the K factor variation at the crack front.

Application

Figure 15 shows an example of application of these results to a C.T. specimen. Parameters are τ_p = 1.5, ΔK_o = 12 MPa $\sqrt{m}$. The major effect of the overload is found on the two surfaces of the specimen (4). Hence the crack front tends to curve when the part of the crack at the interior of the specimen is no longer affected. Calculation (14) indicates that when the crack front is curved the K value at the center of the specimen tends to decrease with respect to the K value at the free surface. Hence, we think, as for elliptical cracks, that crack closure is responsible for the retardation due to overloading. The other effects (acceleration...) are due to a change of the front curvature which affects the K factor values all along the crack front.

CONCLUSION

- Evidence is given that Elber's concept is not limited to the case of propagation under plane stress conditions.
- Crack closure acts for the plane strain condition. In the case of semi-elliptical surface cracks is a gradient of the crack closure stress. This gradient associated with plastic deformation would be responsible for the different evolutions observed for various loading parameters.
- The R-ratio effect in propagation under plane strain is taken into account by a ΔK_{eff} variation.
- The major part of the influence of the stress state can be explained by a difference in the crack closure level.
- ΔK_{eff} variations due to overloading are not limited to plane stress conditions. They must be taken into account for the prediction of two dimensional defects.

SYMBOLS USED

a_o = crack length (or depth) - overload

c = surface crack length

$2r_{yco}$ = cyclic plastic zone size due to baseline load

$2r_{ymp}$ = monotonic plastic zone size due to overload

ΔK_o = stress intensity factor range - overload

ΔK_{eff} = effective stress intensity factor range

U = $\Delta K_{eff}/\Delta K$

τ_p = $\Delta K_{peak}/\Delta K_o$ = overload ratio

REFERENCES

(1) Clérivet, A. and Bathias, C., Eng. Fract. Mech., Vol. 12, No 4, 1979, pp. 599-611.

(2) Elber, W., ASTM-STP 486, 1971, pp. 230-242.

(3) Wheeler, O.E., J. of Basic Eng., ASME, 1972, pp. 181-186.

(4) Clérivet, A., Thesis, Univ. Techn. of Compiegne, France, 1986.

(5) Suresh, Eng. Fract. Mech., Vol. 18, No. 3, 1983.

(6) Schijve, J., Delft Univ. of Techn., Dept. Aeronautical Eng., Report VTH-203.

(7) Bertel, J.D., Clérivet, A. and Bathias, C., ASTM-STP 791, Vol. 1, 1983, pp. I-366-I-379.

(8) Bertel, J.D., Clérivet, A. and Bathias, C., Fatigue Thresholds, Vol. 2, 1982, pp. 1115-1126.

(9) Elber, W., Langley Research Center, Nasa, Report L. 10099, 1975.

(10) McGowan, J.J.and Liu, H.W., Journ. of Eng. Mat. and Techn., Vol. 102, 1980, pp. 341-346.

(11) Jolles, M., Journ. of Eng. Mat. and Techn., Vol. 105, 1983, pp. 215-218.

(12) Newman, J.C., and Raju, I.S., Eng. Fract. Mech., Vol. 105, 1981.

(13) Newman, J.C., and Raju, I.S., Nasa Techn. Memorandum, 83200, 1981.

(14) Labourdette, R., Private communication.

ACKNOWLEDGEMENTS

We would like to thank R. Labourdette (ONERA, FRANCE) for help with numerical calculations.

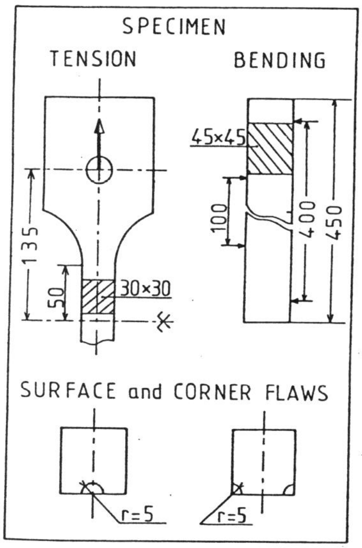

Figure 1 Specimen geometry

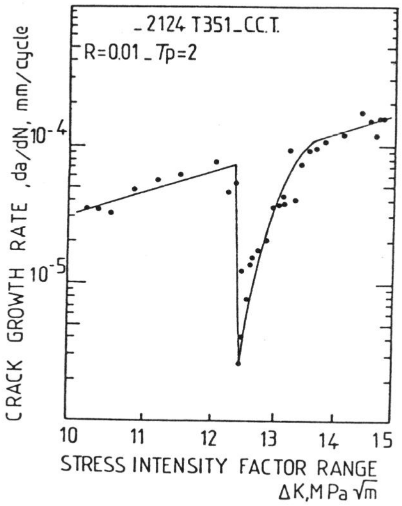

Figure 2 Overloading influence on FCGR – ΔK

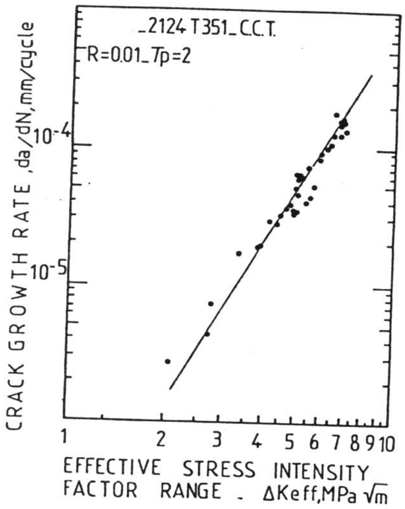

Figure 3 Overloading influence on FCGR – ΔK_{eff}

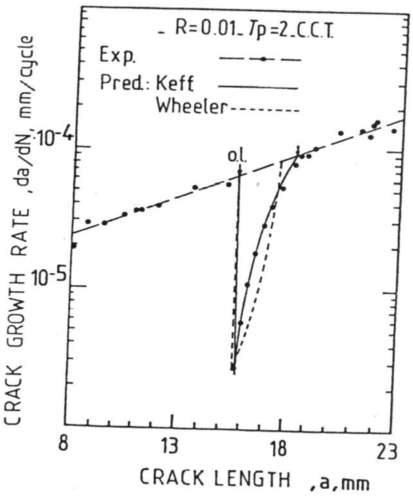

Figure 5 Prediction of retardation due to overloading.

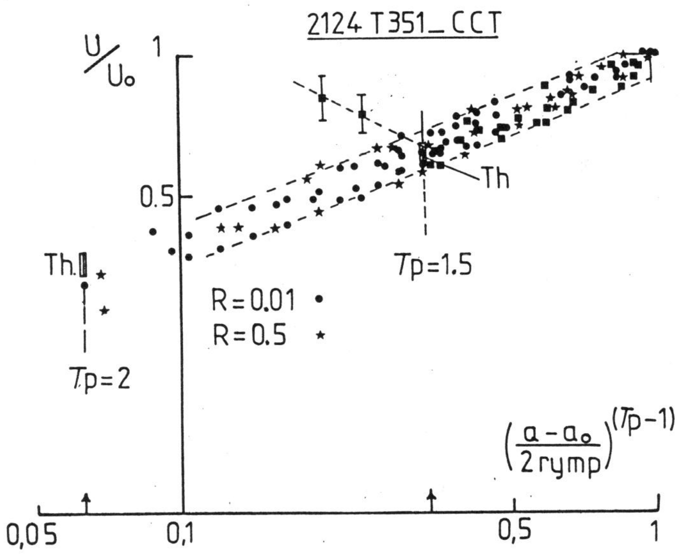

Figure 4 Crack closure and threshold measurements for various overload ratios

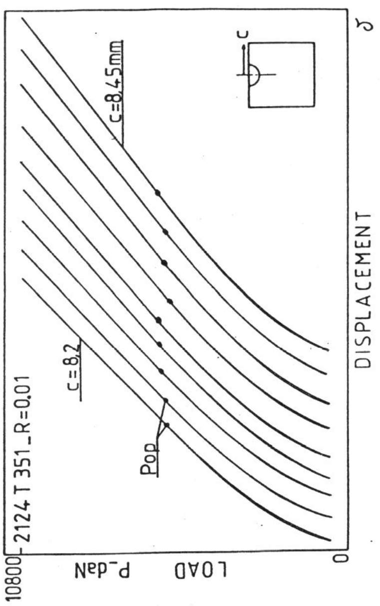

Figure 6 Crack closure determination (surface)

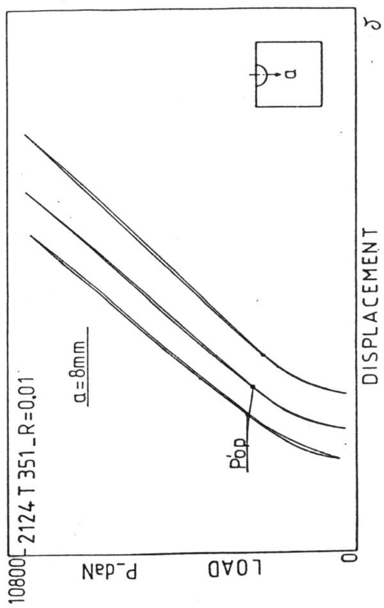

Figure 7 Crack closure determination (interior)

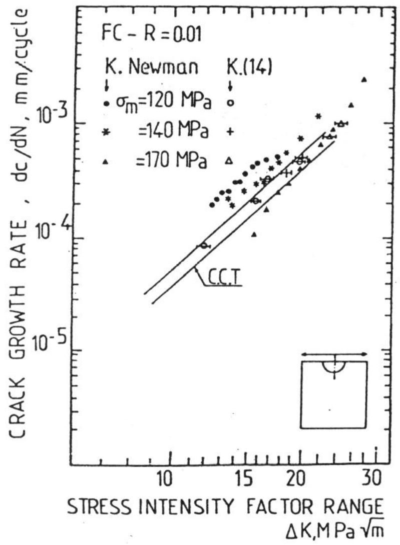

Figure 8 FCGR vs. ΔK-(surface)
K Newman and (14)

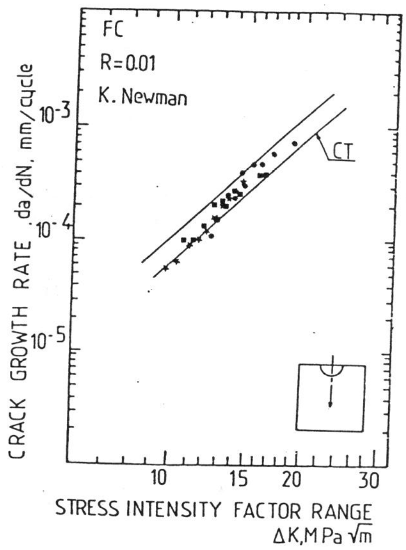

Figure 9 FCGR vs. ΔK-(interior)
K Newman

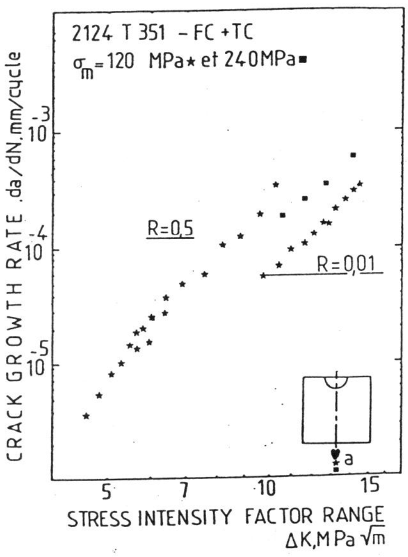

Figure 10 R-ratio influence on
FCGR (interior) vs. ΔK

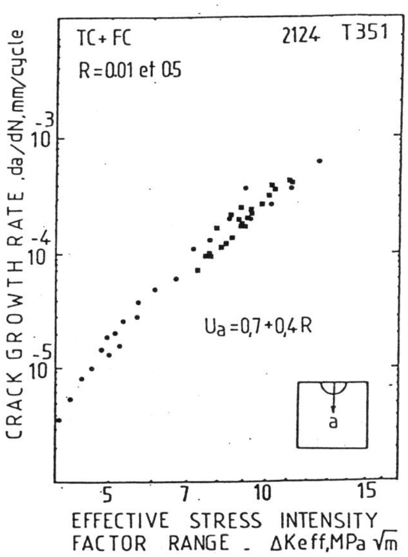

Figure 11 FCGR (interior) vs.
ΔK_{eff} for various R-ratios

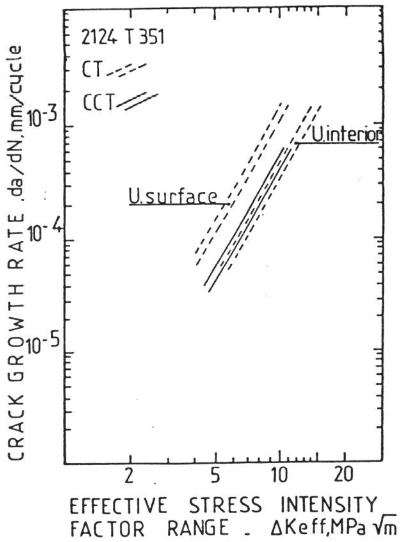

Figure 12 Influence of stress state on FCGR

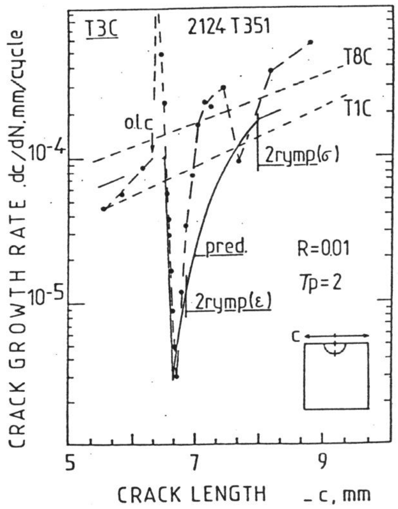

Figure 13 Overload influence - Tension - Prediction

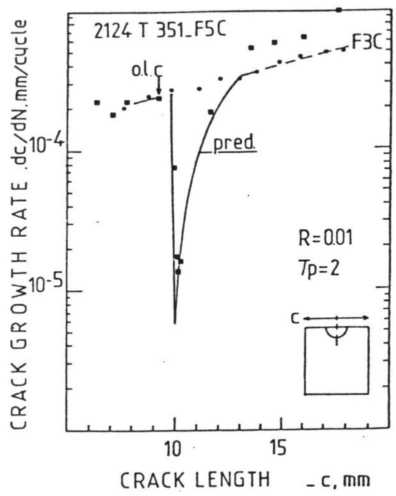

Figure 14 Overload influence - Bending - Prediction

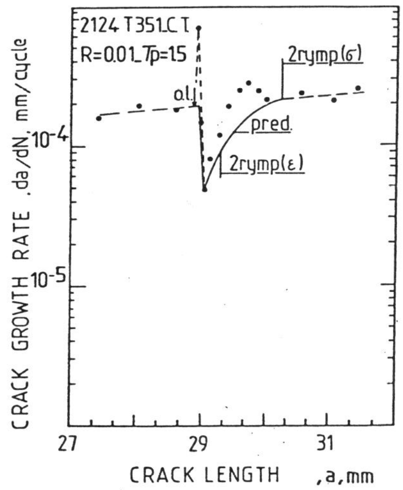

Figure 15 Overload influence - C.T. specimen - Prediction